Dimension Change during Multi-step Imprint Process and In-plain Compression

Miyata, Tsuyoshi
Department of Mechanical and Aerospace Engineering, Kyushu University

Tokumaru, Kazuki
Department of Mechanical Engineering Graduate School of, Kyushu University

Tsumori, Fujio
Department of Mechanical Engineering, Kyushu University

出版情報：Journal of Photopolymer Science and Technology. 33 (2), pp.199-204, 2020-07-01. The Society of Photopolymer Science and Technology(SPST)
バージョン：
権利関係：

Dimension Change during Multi-step Imprint Process and In-plain Compression

Tsuyoshi Miyata[1], Kazuki Tokumaru[1], and Fujio Tsumori[2*],

[1] Dept. Mech. Eng., Grad. School of Kyushu Univ., 744 Motooka, Nishi-ku, Fukuoka 819-0395, Japan

[2] Dept Mech. Eng., Kyushu Univ., 744 Motooka, Nishi-ku, Fukuoka 819-0395, Japan

**tsumori@mech.kyushu-u.ac.jp*

In nature, there are living organisms that have functional properties with a special surface structure. The research has been widely conducted to apply the same functional properties by engineering the above structure. In this study, we focused on the hierarchical structure with high aspect ratio found in lotus leaves and Morpho butterfly scales. We chose Nano imprint lithography (NIL) as a method for fabricating the structures because of its advantages such as low cost and high accuracy. However, the conventional NIL only enables to transfer patterns perpendicular to work surface due to the necessity of mold release, so that we cannot obtain a hierarchical structure by NIL. Therefore, as a new process, we tried to form a hierarchical pattern by multi-step imprinting and to increase the aspect ratio by an in-plane compression method. In this paper, we quantitatively evaluated the interface pattern of each hierarchy.

Keywords: Nano imprint lithography, Multi-scale patterning, Hierarchical structure

1. Introduction

It has been reported that there are species in the natural world that possess functional properties by having a special structure on the surface. For example, lotus shows water repellency on its leaves and Morpho butterflies possess their vivid blue [1]. These characteristics are caused by multi-layered structure on the surface. Nowadays, many scientists and engineers research products with similar functions by mimicking the structures and maneuvers of natural species [2-11]. The present work is also a kind of bio-mimic researches, and focuses on the functional properties like the above-mentioned properties. We tried to reproduce functional surfaces by imitating a hierarchical structure by engineering.

In this study, we used Nano imprint lithography (NIL) as a means to create the surface structure [12-16]. NIL is a processing technology proposed by S. Chou in 1996. It can transfer the mold pattern to resin. The advantages of NIL include its low cost and simple process, which makes it suitable for mass production, and its high resolution. On the other hand, since it is a process using a mold, there is a drawback that it could not transfer a tapered or over-hanging pattern. There are two types of NIL; thermal imprinting is a process for thermoplastic resin and UV imprinting is a process for a UV curable resin. We adopted thermal imprinting in order to use for many kinds of materials.

In this study, we used some processes applying NIL [17-29]. We used NIL's applied technology, multi-layered imprint, which transfers patterns to a sheet in which different materials are layered. In multi-layered imprinting, in addition to being able to transfer to the surface of the work piece, it is also possible to transfer the pattern to the interface between layers at the same time. This is the technology that forms the basis of the multi-step imprint used in this research. Micro powder imprint (μPI), which is a transfer technology that applies NIL to powder metallurgy, can transfer patterns to ceramics and glass compounds. So, it is used to produce fine patterns on ceramic products which are difficult to fabricate patterns by machining. In this experiment, μPI was used to patterns on the layers containing ceramics. In addition, in this study, we propose in-plane compression processing for

imprint moldings with hierarchical patterns [29]. We conducted in-plane compression experiments on moldings that were subjected to multi-layered imprinting in the past, and in consideration of the results, we decided to use it in this study.

The purpose of this research is to develop a processing method that has a higher degree of freedom compared to the conventional method, and to overcome the disadvantage of NIL that the transferable pattern is limited. In previous research, we succeeded in fabricating a hierarchical structure using this method, and confirmed the usefulness of this method [30]. In this paper, in order to discuss the transfer accuracy of the processing method, a quantitative evaluation was performed from the cross-sectional view of the compact after processing.

2. Materials

In this study, an alumina compound sheet was prepared and used as the material to be processed. Fig. 1 (A) illustrates the procedure for preparing the compound sheet. First, after mixing alumina powder (Admafine AO-502, Admatechs), polyvinyl alcohol (PVA, Fujifilm Wako Pure Chemical Industries, Ltd.), glycerin (Wako Pure Chemical Industries, Ltd.), and water. Next, we prepared the slurry by stirring and defoaming. The alumina powder had an average particle size of 0.925 μm, the degree of polymerization of PVA was about 500, and the degree of saponification was 86.0 to 90.0 mol%. Next, using a doctor blade method, the prepared slurry was spread in a uniform thickness on a PET film to form a sheet [31]. After that, it was dried in an oven heated to 70 °C for 900 s to produce a compound sheet. In this study, in order to perform imprinting in a container, it was cut into 20.0 mm squares according to the dimensions of the container. The measurements showed that the thickness of the compound sheet was between 120 and 140 μm.

In this study, we fabricated a sacrificial layer when performing multi-step imprinting. We used a 10 mass% acetone solution of poly (methyl methacrylate) (PMMA, SIGMA-ALDRICH) as the sacrificial layer material. The PMMA had a weight average molecular weight of 350,000 or less.

Figure 2 shows the results of dynamic viscoelasticity measurements on the materials used in this study. It was considered that the influence of humidity was large, so the measurement was performed at a constant humidity of 50 % when measuring the alumina compound sheet.

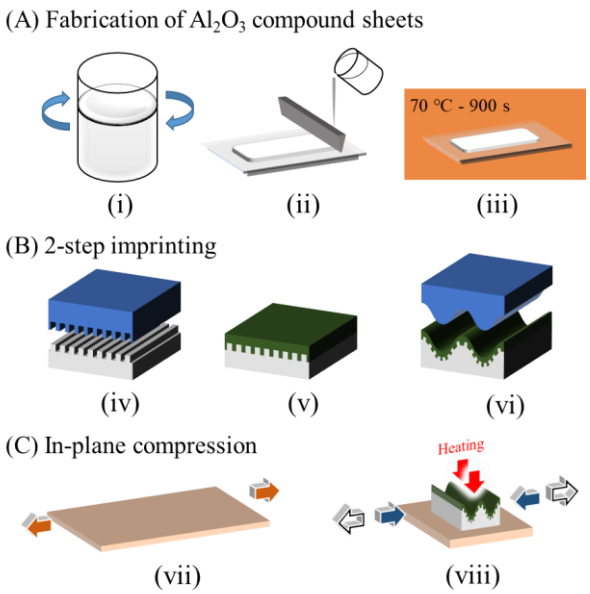

Fig. 1 Flow of the experiment. (i) Preparation of slurry. (ii) Forming into a sheet. (iii) Fabrication of a compound sheet. (iv) 1st imprint. (v) Fabrication of sacrificial layer. (vi) 2nd imprint. (vii) Pre-tension. (viii) Compression due to unloading of tension.

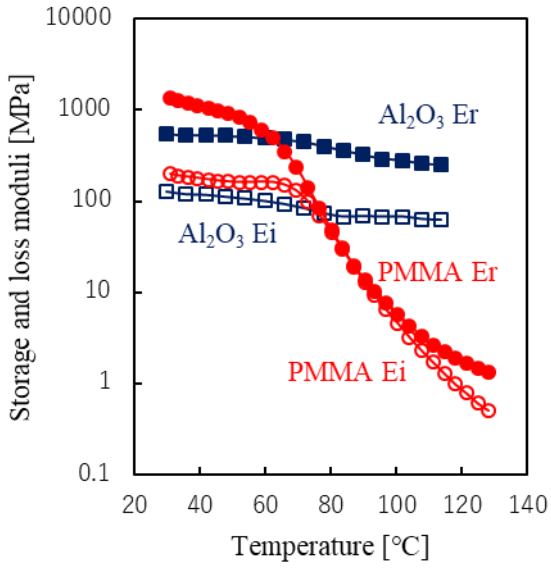

Fig. 2 Storage and loss moduli of the material.

3. Fabrication methods

The processes used in this study are two-step imprinting and in-plane compression [16, 17, 28-30, 32, 33]. Figure 1 (B) shows the procedure for two-

step imprinting, and Fig. 1 (C) shows the procedure for in-plane compression.

First, two-step imprinting is one of the multi-step imprints described in the Introduction, and is a process which two imprints are performed using two types of molds. Before the two-step imprinting, a sample was humidified in a thermo-hygrostat at 30.0 °C and 80 % humidity for a sufficient time. The humidification of the alumina compound sheet was confirmed to improve the machining accuracy, so we decided to humidify it before the work in this study. After humidification, we imprinted a sample in a container heated to 100 °C using a mold with a line and space pattern. The pitch is 10 μm and the depth is 10 μm. In this paper, we call the above imprinting process 1st imprint. After the first imprint, we took the mold and the sample out from the container, placed in a thermo-hygrostat at a temperature of 25.0 °C and a humidity of 50 % for 3.6 ks. After that, we released the mold. Second, we performed spin coating, and formed a liquid film of the sacrificial material shown in Materials on the pattern created by the first imprint. After that, it was dried in an oven heated to 60 °C for 900 s to produce a solid sacrificial layer. After drying, we humidified the sample in a thermo-hygrostat at a temperature of 30.0 °C and a humidity of 80 % for a sufficient time, as before the first imprinting. After humidification, we imprinted the sample in the same container heated to 100 °C using a mold with a waveform pattern with a pattern pitch of 130 μm and a pattern depth of 65 μm. In this paper, we call the above imprint process the second imprint. After the second imprint, when we took the mold and sample out from the container, demolding occurred without applying force.

Next, in-plane compression is a process developed to be applied to imprinted products. In this study, we attempted to increase the aspect ratio of the generated pattern by in-plane compression after two-step imprinting. Before in-plane compression, the sample was humidified in a thermo-hygrostat at 30.0 °C and 90 % humidity. After humidification, we made the rubber substrate stretched according to the compression ratio, and the sample was restrained on the subtrate by the adhesive (SuperX2, Cemedine Co., Ltd.). Relaxing the tension caused the substrate to shrink, causing the sample to compress. In this experiment, we set the compression ratio to 1.5. In this study, we used a 0.5 mm thick silicon rubber sheet (As One Corporation) as a rubber substrate. In addition, since silicone rubber is a difficult-to-bond material, a primer (PPX, Cemedine Co., Ltd.) was applied to facilitate bonding.

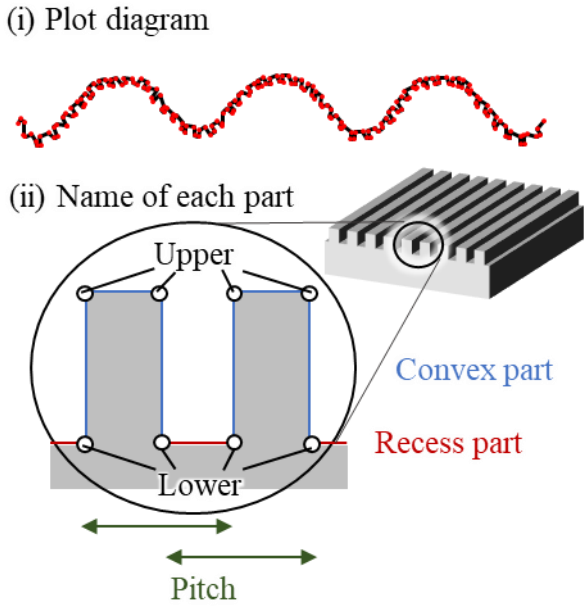

Fig. 3 Schematic of samples. (i) Example of plotting pattern corners. (ii) Diagram for introduction of each part.

In addition, we show the evaluation method of the produced pattern. After processing, the sample with the pattern was cut in the direction in which the pattern could be confirmed, and this section was observed and photographed using a scanning electron microscope (SEM). From the cross-sectional image, the coordinates of the corners of the pattern of the first imprint were plotted as shown in Fig. 3 (i), and the depth and pitch of the first pattern were evaluated. Fig. 3 (ii) shows the names at the time of evaluation. In this paper, we examined the pattern depth, the width of each of the upper and lower parts of the convex and concave parts, and the pitch.

4. Results and discussion

By this processing, the hierarchical pattern shown in Figs. 4 (i) and (ii) was created. Figure 4 (i) is the SEM image after two-step imprinting, and Fig. 4 (ii) is the SEM image after in-plane compression. In this paper, we evaluated the hierarchical pattern after two-step imprinting and after in-plane compression,

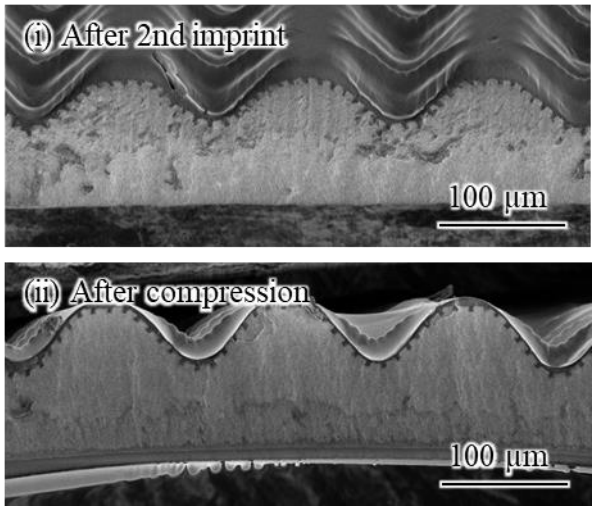

Fig. 4 SEM images of sample cross sections. (i) Image of the sample after 2nd imprint. (ii) Image of the sample after in-plane compression.

and examined the relationship between the dimensions and position of the finer pattern. Figure 4 (ii) shows the sample of Fig. 4 (i) cut out and subjected to in-plane compression. So the conditions for imprinting are the same.

Figure 5 is a distribution diagram showing the relationship between the y-coordinate and the pattern height of the finer pattern, the width of the upper and lower parts of the pattern convex and concave parts, respectively. The y-coordinate is the vertical value on the image, and we set the minimum value of the measured values to 0.

First, comparing the map after the two-step imprint and the map after the in-plane compression processing, it was confirmed that the value after the in-plane compression exists for wider y-coordinate value. This is because the height of the rougher pattern increased due to the increase of the aspect ratio due to the in-plane compression, and a height difference was created.

Second, it was confirmed that the pattern height at the time of the second stage imprint was smaller than the original mold pattern depth of 10 μm. The mold used in this study was a transfer of the original pattern to silicone rubber (two-component RTV rubber KE-1600, Shin-Etsu Chemical Co., Ltd.). So the pattern height was lower than that of the original mold due to the elasticity of the mold. On the other hand, it was not confirmed that the pattern height after in-plane compression was significantly reduced compared to that after two-step imprinting. In addition, the pattern height tended to be constant

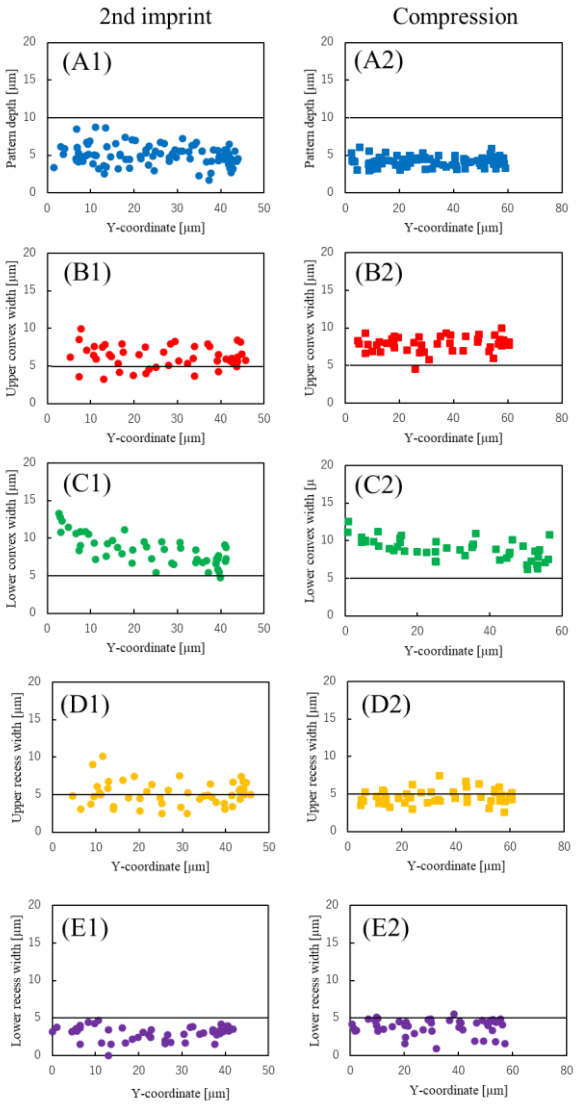

Fig. 5 Distribution diagram showing the relationship between the y-coordinate and some parameters. (A1) and (A2) show the relationship between the y-coordinate and pattern depth. (B1) and (B2) show the relationship between the y-coordinate and upper convex width. (C1) and (C2) show the relationship between the y-coordinate and lower convex width. (D1) and (D2) show the relationship between the y-coordinate and upper recess width. (E1) and (E2) show the relationship between the y-coordinate and lower recess width.

regardless of the position of the finer pattern.

Third, it was confirmed that the width of the pattern convex portion was larger than the original mold width of 5 μm at most the upper parts and all at the lower parts. It was also confirmed that the value after in-plane compression was larger than the

value after two-step imprinting. It is considered that the surface area was increased and the width of the finer pattern was also increased by increasing the height of the rougher pattern due to the in-plane compression processing. In the lower parts, a negative correlation was confirmed between the y-coordinate and the pattern width. This suggests that the increase in surface area mostly caused by in-plane compression may have occurred at the valley of the rougher pattern.

Fourth, the width of the recess part of the patterns at the bottom was often smaller than the original mold width of 5 μm. On the other hand, the value for the upper part is about 5 μm. The reason why the width of the pattern at the bottom of the recess was increased by in-plane compression is thought to be the same as that for the convex part.

Next, Fig. 6 is a distribution diagram showing the relationship between pitch and y coordinate. The pitch is the sum of the width of the protrusion and the width of the recess, and two types of pitch can be measured as shown in Fig. 3 (ii). It was confirmed that the values after two-step imprinting were large at the large and small values of the y-coordinate at both ends of the distribution. This means that the pitch increases near the top and bottom of the rougher pattern. In addition, the increase in pitch due to in-plane compression is considered to be the same as in the case of protrusions.

From the above evaluation, it was confirmed that the deformation of the dimension of the finer pattern due to the in-plane compression was smaller than the deformation caused by the two-step imprint, and did not cause the pattern to be damaged. It was also found that the surface area was likely to increase near the top of the rougher pattern peak and the bottom of the valley from the increase in pitch. In the future, in order to investigate the reproducibility of the above evaluation, we will carry out analysis with FEM and start developing design methods [34].

5. Summary

In this paper, we quantitatively evaluated the newly developed multi-step imprinting method, which is a hierarchical structure manufacturing method, and the in-plane compression processing method, which is a method for increasing the aspect ratio.

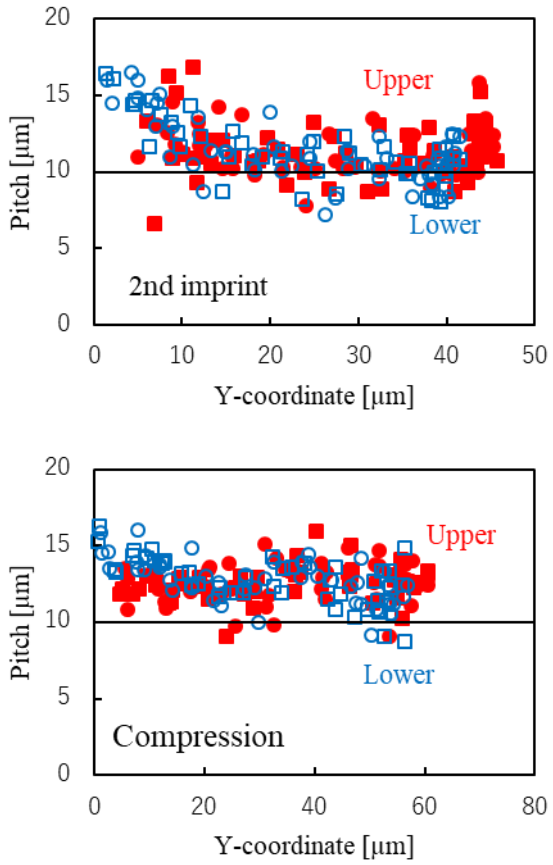

Fig. 6 Distribution diagram showing the relationship between the y-coordinate and pitch.

Acknowledgement

This research is supported by Adaptable and Seamless Technology transfer Program through Target-driven R&D (A-STEP) from Japan Science and Technology Agency (JST). The research is also financially supported by the Mitsui Foundation for the Advancement of Tool and Die Technology.

References

1. S. Kinoshita, S. Yoshioka, and K. Kawagoe, *Proc. R. Soc. B Biol. Sci.*, **269**-1499 (2002) 1417.
2. S. Kinoshita, S. Yoshioka, Y. Fujii, and N. Okamoto, *Forma*, **17** (2002) 103.
3. X. Zhu, W. Yan, U. Levy, N. A. Mortensen, and A. Kristensen, *Sci. Adv.*, **3**-5 (2017) e1602487.
4. W.-G. Bae, H. N. Kim, D. Kim, S.-H. Park, H. E. Jeong, and K.-Y. Suh, *Adv. Mater.*, **26**-5 (2014) 675.
5. H. Lee, B. P. Lee, and P. B. Messersmith,

Nature, **448**-7151 (2007) 338.
6. F. Zhang, J. Chan, and H. Y. Low, *Appl. Surf. Sci.*, **254**-10 (2008) 2975.
7. M. Yoshino, N. Umehara, and S. Aravindan, *Wear*, **266**-5 (2009) 581.
8. P. B. Weisensee, E. J. Torrealba, M. Raleigh, A. M. Jacobi, and W. P. King, *J. Micromech. Microeng.*, **24**-9 (2014) 095020.
9. A. Y. Vorobyev and C. Guo, *J. Appl. Phys*., **117**-3 (2015) 033103.
10. H. Kikuta, *J. Jpn. Soc. Precis. Eng.*, **74**-8 (2008) 781.
11. L. Zhang, Z. Zhou, B. Cheng, J. M. DeSimone, and E. T. Samulski, *Langmuir*, **22**-20 (2006) 8576.
12. S. Y. Chou, P. R. Krauss, and P. J. Renstrom, *J. Vac. Sci. Technol. B*, **14**-6 (1996) 4129.
13. S. Y. Chou, and P. R. Krauss, *Microelectron. Eng.*, **35**-1 (1997) 237.
14. S. Y. Chou, P. R. Krauss, and P. J. Renstrom, *Appl. Phys. Lett.*, **67** (1995) 3114.
15. S. Y. Chou, P. R. Krauss, and P. J. Renstrom, *Science*, **272**-5258 (1996) 85.
16. L. J. Guo, *Adv. Mater.*, **19**-4 (2007) 495.
17. Y. Xu, F. Tsumori, T. Toyooka, H. Kotera, and H. Miura, *Jpn. J. Appl. Phys.*, **50**-6 (2011) 06GK11.
18. F. Tsumori, Y. Tanaka, Y. Xu, T. Osada, and H. Miura, *Jpn. J. Appl. Phys*., **53**-6 (2014) 06JK02.
19. F. Tsumori, S. Hunt, K. Kudo, T. Osada, and H. Miura, *J. Jpn. Soc. Powder Powder Met.*, **63**-7 (2016) 511.
20. F. Tsumori, Y. Xu, Y. Tanaka, T. Osada, and H. Miura, *Procedia Engineer.*, **81** (2014) 1433.
21. F. Tsumori, S. Hunt, T. Osada, and H. Miura, *Jpn. J. Appl. Phys.*, **54**-6 (2015) 06FM03.
22. Y. Xu, F. Tsumori, H. G. Kang, and H. Miura, *Adv. Sci. Lett.*, **12** (2012) 170.
23. F. Tsumori, L. Shen, T. Osada, and H. Miura, *Manuf. Rev.*, **2** (2015) 2015008.
24. Y. Xu, F. Tsumori, H. G. Kang, and H. Miura, *J. Jpn. Soc. Powder Powder Met.*, **58**-11 (2011) 673.
25. Y. Xu, F. Tsumori, T. Osada, and H. Miura, *Micro Nano Lett.*, **8**-10 (2013) 571.
26. F. Tsumori, K. Tokumaru, K. Kudo, T. Osada, and H. Miura, *J. Jpn. Soc. Powder Powder Met.*, **63**-7 (2016) 519.
27. K. Tokumaru, F. Tsumori, K. Kudo, T. Osada, and K. Shinagawa, *Jpn. J. Appl. Phys.*, **56**-6 (2017) 06GL04.
28. K. Yonekura, K. Tokumaru, and F. Tsumori, *Jpn. J. Appl. Phys.*, **57**(2018) 06HG05
29. K. Tokumaru, K. Yonekura, and F. Tsumori, *J. Photopolym. Sci. Technol.*, **32**-2 (2019) 315.
30. T. Miyata, K. Tokumaru, and F. Tsumori, Jpn. J. Appl. Phys. 59 (2020), SIIJ07.
31. K. P. Plucknett, C. H. Caceres, C. Hughes, and D. S. Wilkinson, *J. Ame. Cer. Soc.*, **77**-8 (1994) 2145.
32. Y. Hirai, M. Fujiwara, T. Okuno, Y. Tanaka, M. Endo, S. Irie, K. Nakagawa, and M. Sasago, *J. Vac. Sci. Technol. B*, **19**-6 (2001) 2811.
33. C. H. Lin and R. Chen, *J. Micromech. Microeng.*, **17**-7 (2007) 1220.
34. F. Tsumori, Y. Xu, H. Kang, T. Osada, H. Miura, *Proc. COMPLAS* (2013) 1267.